RSC Advances

PAPER

View Article Online
View Journal | View Issue

Cite this: *RSC Adv.*, 2020, **10**, 2830

The influence of gut microbiota on the rheological characterization of soy hull polysaccharide and mucin interactions

Lina Yang,[ab] Jinghang Huang,[ab] Mingshuo Luo,[ab] Ziyi Wang,[ab] Lijie Zhu,[ab] Shengnan Wang,[ab] Danshi Zhu[ab] and He Liu*[ab]

Nutrients reach the body through the food delivery system, interacting with intestinal mucus and gut microbiota for effective absorption. The purpose of this study was to investigate the possible interactions between soluble soy hull polysaccharide (SSHP), gut microbiota and mucin. The digestive environment of the porcine intestinal mucus was simulated, and the changes of the SSHP–mucin mixed system were monitored by shear rheology, interface measurement, scanning electron microscopy, particle size distribution, and microbial sequencing. First, based on scanning electron microscopy and particle size distribution, it was shown that the gut microbiota undergoes glycolysis in different mucus. The apparent viscosity and viscoelastic properties of the mucus during fermentation were then determined using shear rheology. Compared with the control and microwave-assisted citric acid extraction of soy hull polysaccharide (MCSP), the viscosity of microwave-assisted oxalic acid extraction of soy hull polysaccharide (MOSP) increased significantly ($p < 0.05$) at 24 h, and the thixotropy of all samples increased. The adsorption properties of mucin at the air–liquid interface were analyzed by the interfacial tension technique. As the fermentation time increased, the adsorption performance of the SSHP mucus increased, the interfacial tension decreased, and the expansion modulus increased. Moreover, according to high-throughput 16S rDNA sequencing analysis, the gut microbiota community structure changed significantly after ingestion of MCSP and MOSP, and the abundances of Bifidobacteriaceae and Lactobacillaceae increased to varying degrees. In summary, polysaccharides can be used by the intestinal flora to increase the viscosity and thixotropy of the mucus system, to increase the interfacial strength, and promote the proliferation of intestinal probiotics. This study provides useful insights for the potential application of SSHP.

Received 18th November 2019
Accepted 2nd January 2020

DOI: 10.1039/c9ra09594b

rsc.li/rsc-advances

Introduction

In recent years, the relationship between gut microbiota and human health has become a research hotspot. There is increasing interest in the mechanism of action of gut microbiota in food delivery systems. In the human digestive system, the gut is the main area of nutrient absorption and is closely related to dietary fiber metabolism.[1] Intestinal epithelial cells are covered by a mucous layer that acts as a defensive barrier against toxic compounds, bacteria, and viruses, while allowing nutrients to diffuse to the epithelial surface and provide lubrication for the food through the gut.[2] Mucus consists mainly of water (95% w/w) and mucin (about 5% w/v).[3] Mucin is a high molecular weight glycoprotein produced by goblet cells and is responsible for the rheological properties of mucus.[4] Studies have shown that proteins and polysaccharides have a high affinity for electrostatic interactions, which may cause physical changes in the mucus layer.[5] Polysaccharides may form a similar polysaccharide–mucin complex in the intestinal digestive delivery system, affecting the release and absorption of nutrients. The interfacial dilational rheology method was used to study the interfacial properties of nutrient diffusion in mucus.[6] When the molecules were rearranged and the conformation changed at the interfacial interface, the dynamic and mechanical properties of the interfacial layer changed, increasing our understanding of the mechanism of nutrient digestion and absorption in the food delivery system.

The nutrient sources in the diet include a variety of glycans derived from plants and animals, most of which cannot be digested and absorbed by the host's digestive tract. However, the gut microbiota colonized in the large intestine can secrete enzymes that degrade complex carbohydrates such as polysaccharides.[7] *Bacteroides* is the main degrader of

[a]*College of Food Science and Technology, Bohai University, 19 Keji Road, Songshan New Region, Jinzhou, Liaoning, 121013, China. E-mail: liuhe2069@163.com; Tel: +86 13464319258*

[b]*National & Local Joint Engineering Research Center of Storage, Processing and Safety Control Technology for Fresh Agricultural and Aquatic Products, Jinzhou, Liaoning, 121013, China*

polysaccharides, and its genome encodes more glycoside hydrolase and polysaccharide lyase genes. Some bacteria of the Firmicutes and *Bifidobacterium* in the Actinomycetes can also metabolize certain glycans.[8] At the same time, the localization and metabolism of mucin by gut microbiota is beneficial to the host, which can stabilize the intestinal community and promote mucin secretion and barrier function.[9]

In this study, we used shear rheology to evaluate the effects of changes in mucus structure and composition caused by the interaction of gut microbiota and nutrients on basic rheological properties. In order to further research the interaction between nutrients and mucus at the molecular level, interfacial dilational rheology was employed to characterize the properties of the interface mixed with mucus dispersion. The changes in gut microbiota were investigated during simulated digestion *in vitro* by high-throughput amplicon sequencing. Meanwhile, we also evaluated the role of the gut microbiota in the SSHP–mucin system. This work points out the complexity and importance of the SSHP-mucus interaction, suggesting that intestinal mucus may play a role that cannot be ignored in nutrition intake. It also provides useful insights into the effects of gut microbiota on nutrient delivery systems.

Materials and methods

Materials

Soy hulls were obtained from Yu Wang Group of Shan Dong in China. All chemical reagents used were analytical grade. Deionized water was used throughout.

Porcine intestinal mucus extraction

Porcine mucus was prepared as described previously.[10] Fresh porcine large intestines were obtained from local slaughterhouses, divided into approximately 15 cm, and washed with 0.01 M phosphate-buffered saline (PBS) isotonic buffer large intestine. The mucous was then squeezed by hand to the surface to separate the mucus, which was carefully scraped and collected, and the protease inhibitor Cocktail (MedChemExpress, USA) was added at 100 : 1 (v/v).

Soy hull polysaccharides extraction

According to our previous study,[11] the soy hull powder was dissolved in 10-times volumes of 1% (v/v) ethanol and stirred for 30 min. Then, the mixture was filtered and the residue was dried at 65 °C. Subsequently, 50 g of the soy hull residues were extracted in 20-times volume of 0.6% (w/v) oxalic acid or citric acid with microwave (WD800G, Glanz, Guangzhou, China) assistance for 35 min at 480 W. After cooling and filtering, the extracts were centrifuged at 1500 × *g* (TDL-5-A, Anke, Shanghai, China) for 15 min. Subsequently, the supernatant was concentrated using a rotary evaporator (RE-3000A, Yarong, Shanghai, China) and precipitated with two volumes of ethanol for 40 min. After filtration, the precipitate is dried at 65 °C, generating two SSHP samples (microwave-assisted oxalic acid extracted soy hull polysaccharide, MOSP. microwave-assisted citric acid extracted soy hull polysaccharide, MCSP).

In vitro simulated digestion

The mucin content was determined by the bicinchoninic acid protein (BCA) assay kit to be 2.803 ± 0.024 mg mL^{-1}. The mucus was diluted with PBS (0.01 M) buffer to give a final protein concentration of 0.6 mg mL^{-1}. The MOSP or MCSP solution was added to the mucus at a concentration of 10 mg mL^{-1}, and mucus without SSHP was used as a control sample. Fresh feces were mixed in equal proportions from three healthy volunteer without any gastrointestinal diseases and antibiotic therapy in the past half year and added to a sterile 0.01 M PBS (pH 7.4) to prepare a stool slurry, which was added to the culture system at a ratio of 1 : 10 and cultured at 37 °C for 48 h in an anaerobic incubator (90% N_2, 5% H_2 and 5% CO_2) (LAI-3, Longyue, Shanghai, China).

The DNA of original and cultured gut microbiota (GM) was extracted according to manufacturer's instructions QIAamp Fast DNA Stool Mini Kit (QIAGEN, Germany). The V3–V4 region of the 16S rDNA gene fragments was amplified using a set of primer pairs (341F: 5′-CCCTACACGAC GCTCTTCCGATCTG (barcode) CCTACG GGNGGCWG CAG-3′, 805R: 5′-GACTGGAGTTCCTTGGCACCCGA-GAATTCCAGACTACHVGGGTATCTAATCC-3′). Statistical analysis of biological information is typically performed at operational taxonomic units (OTUs) at 97% similar levels.

Determination of carbohydrate

In order to verify whether SSHP can be used as a substrate for the growth and reproduction of gut microbiota, we took samples at 0 h, 24 h and 48 h to identify the total carbohydrates, reducing sugar and uronic acid content. The mucus was centrifuged at 4000 rpm for 10 min to obtain a supernatant. The total carbohydrates content was determined by the phenol–sulfuric acid method using glucose as standard.[12] Take 0.5 mL of the supernatant, add 0.5 mL of a 5% phenol solution and 2.5 mL of H_2SO_4, and bath in 30 °C water for 20 min, and measure the absorbance at 490 nm. The DNS method was used to determine the reducing sugar content using glucose as standard.[13] Take 1 mL of the supernatant, add 1 mL of DNS reagent, and bath in boiling water for 5 min. After cooling, add 8 mL of deionized water and measure the absorbance at 540 nm. The uronic acid content was determined by carbazole–sulfuric acid colorimetry using galacturonic acid as standard.[14] Take 2 mL of the supernatant, add 12 mL of H_2SO_4, and bath in boiling water for 10 min. After cooling, add 1 mL of a 1.5 g L^{-1} carbazole solution, and measure the absorbance at 530 nm.

Scanning electron microscopy (SEM)

The surface and microstructure of mucus at 0 h, 24 h and 48 h were observed by SEM (S-4800 scanning electron microscope, Hitachi Limited, Japan) at 3.0 kV. The dry samples were placed on metal disk using double-face conducting adhesive and coated with a gold layer. Representative micrographs were taken for each sample at 9000 magnification.

Particle size distribution

According to the principle of dynamic light scattering, the particle size analyzer (90Plus Zete, Brookhaven instruments,

USA) was used to determine the effective diameter of different mucus in anaerobic culture for 0 h, 24 h and 48 h. Parameter setting: scattering angle 90°, laser wavelength 640 nm, temperature 37 °C, particle refractive index 1.59, solvent water, solvent refractive index 1.33.

Shear rheology analysis

Rheological analysis of mucus at 0 h, 24 h and 48 h of anaerobic fermentation was carried out using a rotational rheometer (Discovery HR-1, TA instrument, USA). The sample was loaded onto a rheometer plate (parallel-plate geometry, diameter 40 mm, gap 50 μm), linear shear at 37 °C, shear rate 0.01–1000 s^{-1}, measurement time 300 s, continuous measurement 30 data points were used to test the apparent viscosity of the sample as a function of shear rate. Next, the shear rate was linearly increased from 0.01 s^{-1} to 100 s^{-1}, and 30 data points were collected for 150 s. Linearly reduced from 100 s^{-1} to 0.01 s^{-1}, 30 data points were collected for 150 s to monitor the thixotropic properties of mucus. The exposed sample surface at the plate edge was covered with a thin layer of light silicone oil to prevent moisture loss during rheological tests.

Dynamic interfacial tension measurements and dilational rheology

The mucus interfacial tension (π) and the dilational modulus (E) at the air–liquid interface were studied using a video optical contact angle meter (OCA25, Dataphysics, Germany). The method was modified according to Guri *et al.*[6] and Li *et al.*,[15] the sample injector (inner diameter, 1.83 mm) automatically formed a droplet of 10 μL volume at the tip, placed in a glass cuvette containing the same mucus, covered with a parafilm, thereby reducing moisture volatilization on the measurement results influences. Based on the Young–Laplace equation, the interfacial tension and dilational modulus of the air–liquid interface were measured within 3000 s. The droplet underwent a sinusoidal oscillation at a fixed frequency (0.1 Hz) with a strain amplitude of 0.1 ($\Delta A/A = 0.1$ and A is the droplet surface area). The strain amplitude was predetermined to be within the linear viscoelastic range.

Statistical analysis

The data analysis utilized multiple comparisons performed using SPSS 19.0 software. All of the experiments were conducted in triplicate, and the data are expressed as mean ± SD. A value of $p < 0.05$ was considered to indicate statistically significant difference.

Results and discussion

Changes in total carbohydrates, reducing sugar, and uronic acid

As shown in Table 1, the total carbohydrates content of the three groups gradually decreased as the culture time was extended. After 24 h of fermentation, the total carbohydrate content of MCSP and MOSP samples was significantly decreased ($p < 0.05$). With increased time, the reducing sugars and uronic acid of the three groups of samples showed a trend of increasing first and then decreasing. There was no additional sugar source in the control group, so the initial values were lower than the other two groups. Polymer dietary fiber such as polysaccharides can be metabolized and used as an energy source for the growth and reproduction of gut microbiota. Therefore, as the culture time increased, SSHP was continuously consumed, and the total carbohydrate concentration was gradually reduced. After microbial fermentation, the glycosidic bonds of MCSP and MOSP were destroyed, which was accompanied by a large amount of reducing sugar and uronic acid production. In the subsequent fermentation process, the reducing sugar and uronic acid were directly used by the gut microbiota, so the concentration was decreased. It can be seen that SSHP can serve as a substrate for the growth and reproduction of intestinal microorganisms. Li *et al.*[16] artificially simulated the gastrointestinal model to digest wheat germ polysaccharides. The results showed that the reducing sugar concentration increased significantly from 0.0039 ± 0.0007 mg mL^{-1} to 0.0604 ± 0.0001 mg mL^{-1} after simulated digestion for a period of time. Wang *et al.*[17] simulated human gut microbiota digestion of coral polysaccharides *in vitro*. The result showed that the concentration of reducing sugar decreased from 0.954 ± 0.038 mg mL^{-1} to 0.202 ± 0.003 mg mL^{-1} after 24 h of fermentation, and the total carbohydrates content decreased from 67.84 ± 1.17% to 30.76 ± 5.25%.

Table 1 Changes in total carbohydrates, reducing sugar and uronic acid content in mucus (mg mL^{-1}). Different letters represent significant differences in the same group at different fermentation times ($p < 0.05$)

Fermentation time		Total carbohydrates	Reducing sugar	Uronic acid
Control	0 h	0.332 ± 0.066^{a}	0.156 ± 0.011^{b}	0.039 ± 0.003^{b}
	24 h	0.281 ± 0.011^{a}	0.223 ± 0.011^{a}	0.055 ± 0.009^{a}
	48 h	0.137 ± 0.021^{b}	0.171 ± 0.008^{b}	0.036 ± 0.002^{b}
MCSP	0 h	0.731 ± 0.014^{a}	0.192 ± 0.006^{b}	0.053 ± 0.002^{b}
	24 h	0.603 ± 0.052^{b}	0.297 ± 0.021^{a}	0.243 ± 0.017^{a}
	48 h	0.267 ± 0.049^{c}	0.208 ± 0.008^{b}	0.175 ± 0.004^{b}
MOSP	0 h	0.727 ± 0.065^{a}	0.197 ± 0.020^{b}	0.061 ± 0.005^{c}
	24 h	0.568 ± 0.029^{b}	0.302 ± 0.041^{a}	0.276 ± 0.019^{a}
	48 h	0.234 ± 0.005^{c}	0.213 ± 0.003^{b}	0.246 ± 0.030^{b}

Microstructure and particle size distribution

Fig. 1a shows the microstructure of intestinal juice at different incubation times using scanning electron microscopy (SEM). As the fermentation progressed, the 0 h control exhibited network structure and irregular massive particles. The morphological structure of the 0 h MCSP was irregular and blocklike, with spherical or rod-like particles on the surface, while the 0 h MOSP has a crosslinked porous structure, with massive particles scattered within it. According to previous studies, different extracting agents affect the spatial conformation of polysaccharide aqueous solutions. MCSP has a circular conformation, while MOSP exhibits a helical conformation, which causes microscopic structure differences. Likewise, the monosaccharide composition of MCSP and MOSP are different.

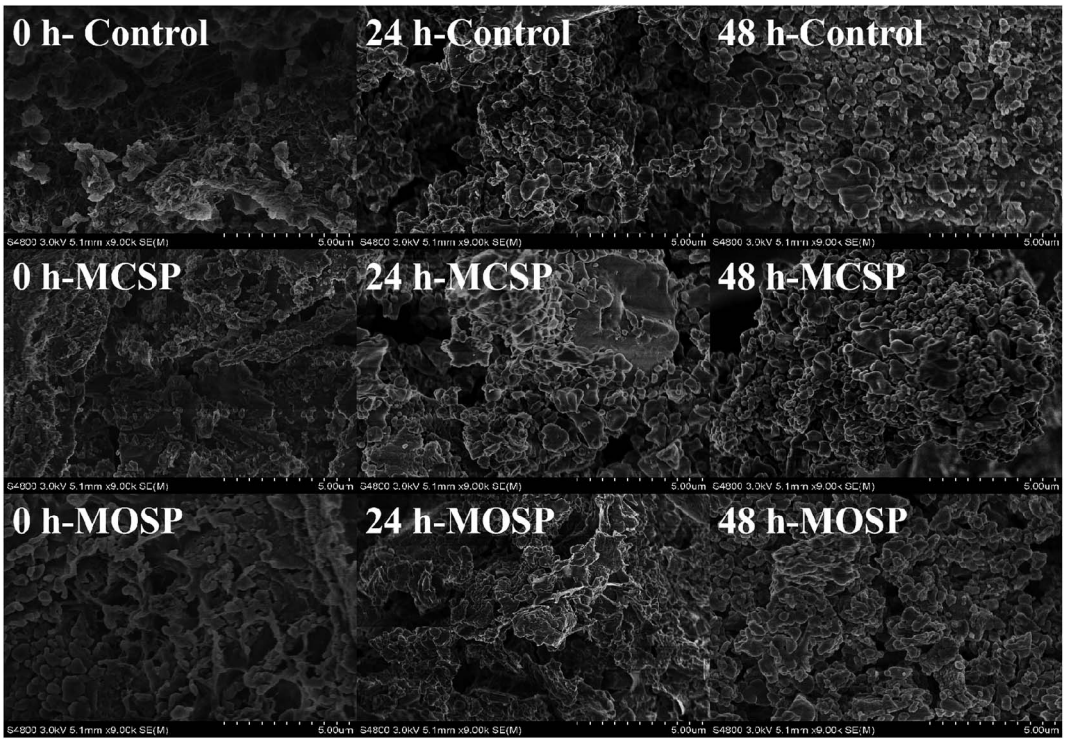

Fig. 1 Microstructure of mucus *in vitro* (×9000). SEM images of control, MCSP and MOSP at 0, 24 and 48 h.

Rhamnose and xylose are absent in MCSP, and the molecular weights of the two are also different. MCSP is significantly larger than MOSP ($p < 0.05$).[18] Liu[19] compared the bioactivity of three polysaccharides (GLP-1, GLP-2, and GLP-3) purified from *Grateloupia livida*. SEM images showed significant differences in the surface characteristics of the three polysaccharides, and GLP-2 as an anticoagulant was superior to GLP-1 and GLP-3 in its antioxidant activity. Therefore, the different microstructures of polysaccharides were closely related to differences in physicochemical properties and biological activities. After 24 h of fermentation, the mucin was consumed by gut microbiota with the structure of the polymer network disappearing and particles increasing because no other carbon source was added to the 24 h control. The irregular mass of 24 h-MCSP was degraded by the gut microbiota, and its main structure was replaced by spherical or rod-shaped particles. The microstructure of the 24 h MOSP had a partial network structure, which may have resulted from the microbiota preferentially utilizing SSHP in a nutrient-rich medium. At the end of the fermentation (48 h control, 48 h MCSP, and 48 h MOSP), all microstructures of the samples appeared as aggregated spherical and rod-shaped particles, which may have been due to the degradation of proteins and polysaccharides in the mucus by the bacterial community.

Mucus particle size is an important indicator of digestive products, which directly affects the rheological properties and digestive properties.[20] The polydispersity index (PDI) corresponding to effective diameter was between 0.07 and 0.80, indicating that the particle distribution of the measurement system was uniform. It can be seen from Table 2 that the equivalent particle size of the fermentation product in the control, MCSP, and MOSP samples gradually decreased with increased fermentation times. At the beginning of fermentation (0 h), the effective diameter of MCSP was significantly greater than that of the control and MOSP ($p < 0.05$).[18] According to a previous study, the particle size of the MCSP solution was significantly larger than that of the MOSP solution ($p < 0.05$).[18] The reason for this difference may be that the different extracting agents led to different molecular weights of SSHP and affected its particle size distribution. As the fermentation progressed, the effective diameter and PDI of the three groups of samples decreased significantly ($p < 0.05$). The diameter of particles in mucus reduced and the distribution range of

Table 2 Particle size and the polydispersity index of mucus at different fermentation time. The different uppercases represent significant differences in the different group at the same time ($p < 0.05$). The different lowercases represent significant differences in the same group at different time ($p < 0.05$)

Sample		Effective diameter (μm)	PDI
Control	0 h	0.863 ± 0.033^{Ba}	0.301 ± 0.013^{Ba}
	24 h	0.604 ± 0.042^{Bb}	0.217 ± 0.028^{Bb}
	48 h	0.508 ± 0.08^{Ab}	0.185 ± 0.030^{Ab}
MCSP	0 h	4.625 ± 0.076^{Aa}	0.532 ± 0.028^{Aa}
	24 h	0.763 ± 0.024^{Ab}	0.286 ± 0.008^{Ab}
	48 h	0.551 ± 0.054^{Ab}	0.209 ± 0.007^{Ac}
MOSP	0 h	1.042 ± 0.085^{Ba}	0.309 ± 0.017^{Ba}
	24 h	0.726 ± 0.045^{Ab}	0.284 ± 0.020^{Aa}
	48 h	0.531 ± 0.060^{Ac}	0.181 ± 0.040^{Ab}

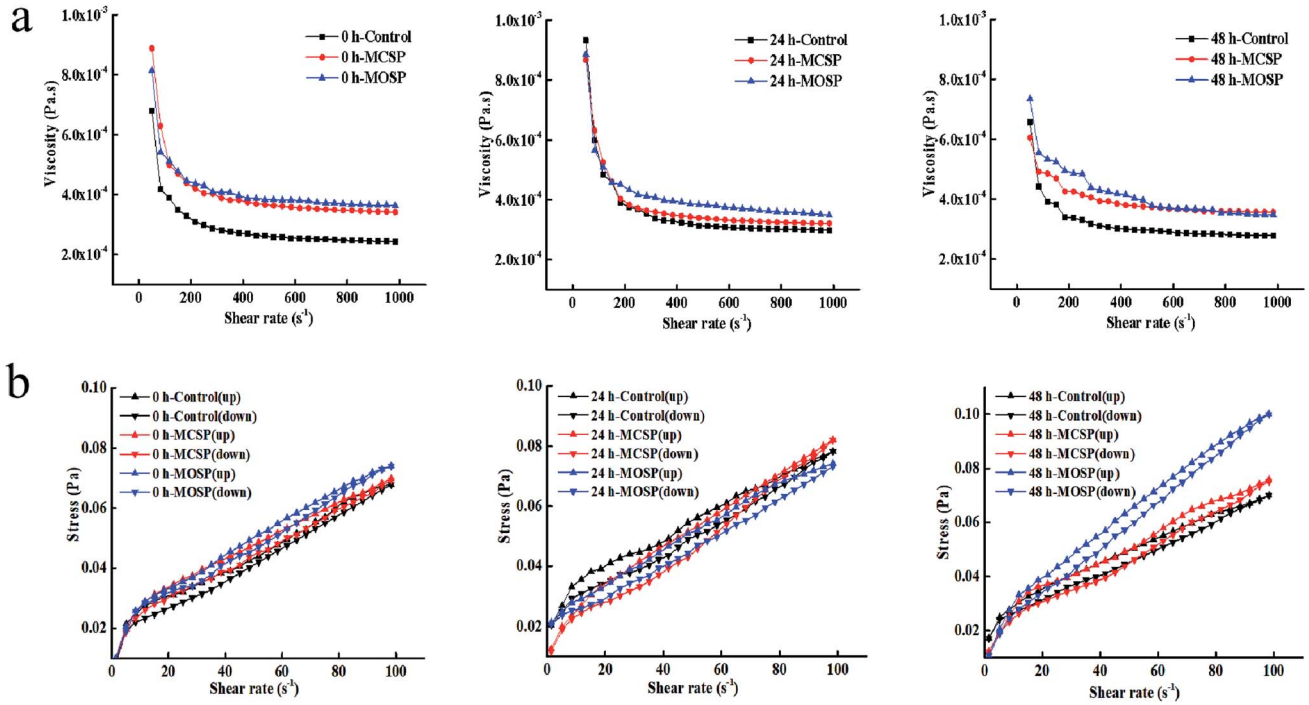

Fig. 2 Effect of SSHP on shear rheological properties of mucus. (a) Dependence of the apparent viscosity on the shear rate at 0, 24 and 48 h. (b) Dependence of the stress on the shear rate (mucus thixotropy) at 0, 24 and 48 h.

particle size decreased. Table 1 shows that the macromolecular polysaccharide was degraded into small molecular reducing sugars and uronic acid in the gut microbiota between 0–24 h, and the mucin was also degraded as a nitrogen source to cause a significant decrease in the particle size. By the end of the fermentation (48 h), the effective diameter of the three groups of samples tended to be consistent due to the consumption of nutrients in the mucus.

Shear rheological properties

The rheological properties of intestinal mucus are important parameters of the intestinal barrier. The changes usually affect the colonization, distribution, and growth of the intestinal flora, and thus affect the absorption of nutrients and drugs.[4] The apparent viscosity of different fermented mucilits was determined at a shear rate of 0.01–1000 s^{-1}. Fig. 2a shows that all samples were pseudoplastic fluids. The rule of shear thinning and solidification characteristics is similar to the actual rheological properties of human intestinal mucus.[21,22] Henry[23] found the apparent viscosities of the three concentrations of chia seed mucus before and after digestion were proportional to the concentration and decreased with an increase of shear rate, showing the characteristics of shear thinning at 37 °C at a shear rate of 0.01–300 s^{-1}. Nikolay[24] showed the shear thinning behavior of four dietary fiber solutions at high concentrations. As the concentration of dietary fiber increased, the intensity of shear thinning behavior became more obvious at a shear rate of 0.01–1000 s^{-1} at 37 °C. Table 3 shows that there was no significant difference in viscosities between the three groups of mucus samples at 0 h. The viscosity of the MOSP mucus at 24 h was significantly higher than the MCSP and control mucus samples. It may be that the gut microbiota makes rapid use of MOSP within 0–24 h, and the metabolites produced are different from MCSP and control, thus increasing the viscosity of mucus. The viscosity of MOSP and MCSP mucus decreased and was kept constant for 48 h, possibly because the gut microbiota fermentation approached the end point and the differences in fermentation end products were small. Previous studies have shown that the increase in viscosity is conducive to the proliferation of anaerobic bacteria, while the proliferation of gut microbiota will also increase the viscosity of the culture system.[25]

Table 3 Power law model fitting parameters of control, MCSP and MOSP at different fermentation time. K is the consistency coefficient, which is equivalent to the viscosity measurement. n is the flow index, when $n < 1$, it is a pseudoplastic fluid, and the value of n indicates the degree of fluid deviation from Newtonian fluid. Different letters represent values of different samples at the same time are significant ($p < 0.05$)

Fermentation time		K (mPa s^n)	n	R^2
0 h	Control	0.761 ± 0.004^{a}	0.832 ± 0.009^{b}	0.989
	MCSP	0.852 ± 0.031^{a}	0.851 ± 0.029^{ab}	0.994
	MOSP	0.799 ± 0.073^{a}	0.882 ± 0.015^{a}	0.972
24 h	Control	0.907 ± 0.061^{b}	0.823 ± 0.033^{a}	0.952
	MCSP	0.999 ± 0.070^{ab}	0.815 ± 0.053^{a}	0.949
	MOSP	1.251 ± 0.238^{a}	0.800 ± 0.038^{a}	0.959
48 h	Control	0.831 ± 0.054^{a}	0.811 ± 0.048^{a}	0.971
	MCSP	0.856 ± 0.012^{a}	0.798 ± 0.043^{a}	0.959
	MOSP	0.889 ± 0.028^{a}	0.855 ± 0.025^{a}	0.988

The thixotropy fluid formed a network structure inside the fluid due to the physical agglomeration or electrostatic attraction of the internal molecules.[26] Under the action of external forces, the bond structure between particles was destroyed, and the microscopic network structure changed with a change of shear rate, which presented as shear thinning or shear expansion on the macro level.[27] Fig. 2b shows that the mucus of the control, MCSP, and MOSP samples formed a thixotropic ring from 0 h to 48 h. The thixotropic ring areas of the control, MCSP, and MOSP samples were 0.27 Pa s^{-1}, 0.29 Pa s^{-1}, and 0.22 Pa s^{-1}, respectively at 0 h. There was no significant difference between the three samples. The thixotropic ring areas of the control, MCSP, and MOSP samples were 0.34 Pa s^{-1}, 0.46 Pa s^{-1}, and 0.44 Pa s^{-1}, respectively at 24 h. With increased fermentation times, the gut microbiota destroyed the structure of the mucus and the thixotropy increased. MCSP and MOSP treatment changed the thixotropy of the mucus due to the elevated viscosity of the system after the polysaccharide was fermented by gut microbiota. At 48 h, thixotropic ring areas were 0.32 Pa s^{-1}, 0.42 Pa s^{-1}, and 0.43 Pa s^{-1}, respectively. The area of the thixotropic ring represents the recovery rate of the mucus structure, and the smaller the area, the weaker the thixotropy.[28] The comparison results showed that the control group had faster reconstruction and better rheological stability. Ellen[29] studied the rheological characterization of culture broth containing the exopolysaccharide, PS-EDIV, from *Sphingomonas pituitosa*. Because the polymer bundles were arranged in the direction of rotation after shearing, the estimated viscosity when the shear rate decreased was lower than that it actually increased. Alicia[30] studied the rheological behavior of an original solution of *Protochaete flavosporus* in the degradation of lignin. The results showed that thixotropy increased with increased fermentation times in a medium containing lignin.

Effects of MCSP and MOSP on interfacial dilational properties of mucus

Interfacial dilational properties. The dispersion characteristics of polysaccharides in mucus during *in vitro* simulation were studied using drop-shaped tension measurements. Fig. 3a shows that the interfacial tension of all samples decreased with time and reached a stable value. At the initial fermentation, the rates of interfacial tension reduction in the MCSP and MOSP groups were slightly slower than that in the control group, showing that the adsorption rate of mucin at the interface was slower than that of the control group. At the same time, the interfacial tension values of MCSP and MOSP were higher than those of the control group, because the viscosities of MCSP and MOSP were greater than the viscosity of the control sample (Fig. 2), so it may have hindered the molecular motion in the mixed system, thereby reducing the adsorption rate of mucin. According to our previous study, the molecular weight of MCSP was significantly larger than the molecular weight of MOSP ($p < 0.05$), so the difference in molecular weight may cause the interfacial tension of MCSP to be less than that of MOSP.[31] As the fermentation time increased (Fig. 4b and c), the results of Table 2 showed that the particle size distribution of the three groups of mucus samples significantly decreased within 24 h of fermentation ($p < 0.05$), and the gut microbiota continued to utilize nutrients. Polysaccharides or proteins are broken down into monosaccharides, polypeptides, and amino acids. They

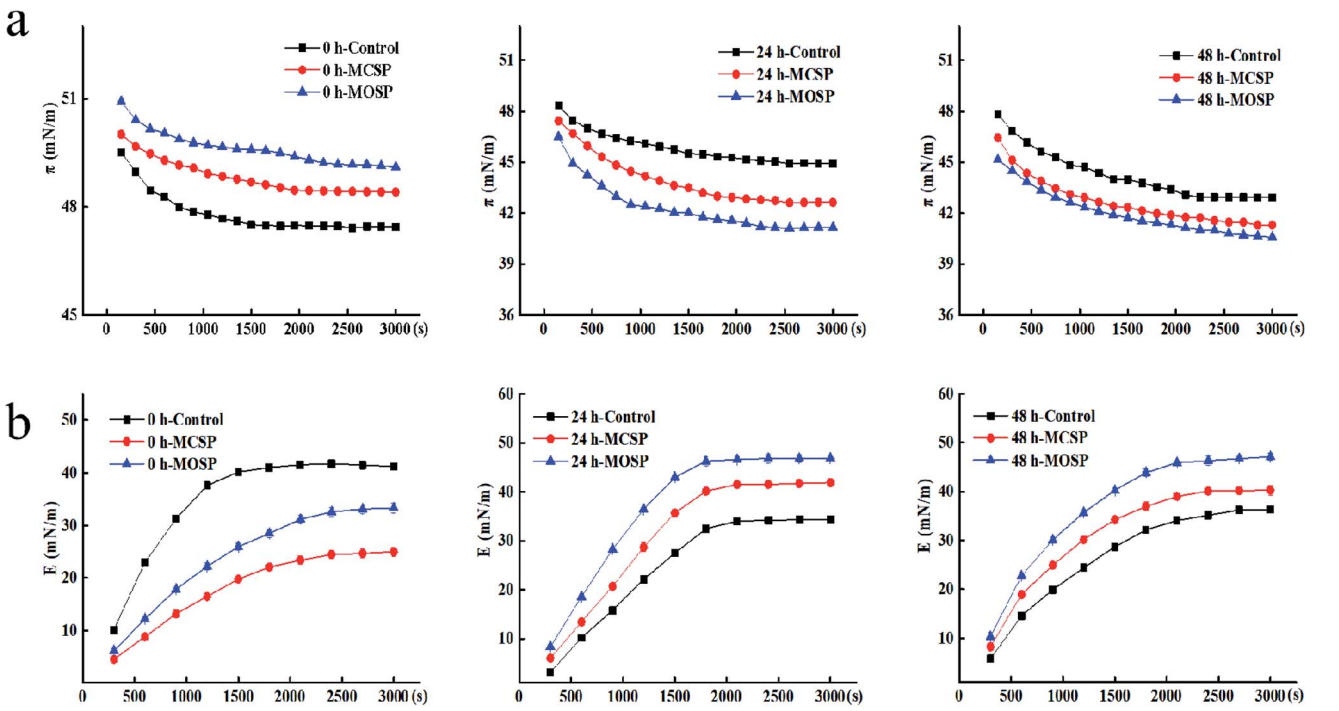

Fig. 3 Effect of SSHP on the interfacial dilational properties of mucus. (a) Interfacial tension (π) of mucus at 0, 24 and 48 h during the measurement time of 3000 s. (b) The dilational modulus (*E*) of mucus at 0, 24 and 48 h during the measurement time of 3000 s.

have little effect on the viscoelastic properties of the mucus interface, and the competitive adsorption and steric hindrance effects on the protein are weakened, which is beneficial for the diffusion of mucin in the system to further rearrange at the interface, resulting in a decrease in interfacial tension. The mucin in the control sample was consumed by the flora, so its interfacial tension value increased. At the same time, the adsorption rate of the control sample was slower than that of MCSP and MOSP, and it had a higher interfacial tension platform, indicating that there was still a large amount of mucin in the mixed system with added SSHP, when compared with the control group.

To further understand the interaction between polysaccharide and mucus at the air–liquid interface, we determined the change of the dilational modulus of the mucus interface at different fermentation times during a measurement time of 3000 s. Fig. 3b shows that the *E* value of all the samples gradually increased with an increase of the adsorption time, which was the inevitable result of the adsorption of the surface active material at the interface, and the *E* values tended to be stable at the equilibrium of adsorption. At the initial stage of fermentation, the *E* value of the three groups of samples gradually increased with increased measurement times, and the *E* value of the final 0 h control sample was higher than that of MCSP and MOSP samples. There may be two reasons for this trend. First, the protein adsorption interface in the mixed system may bind to protein with SSHP by covalent bonds or electrostatic actions, forming adsorption competition between the protein–polysaccharide composite adsorption layer or complex and protein, replacing protein adsorption on the interface. The system was complex, leading to multilayers of protein conformation and weakened interactions between proteins. Second, there was steric hindrance of polysaccharides, so that proteins could not be closely rearranged, resulting in less interaction between proteins at the contact interface. In summary, protein adsorption and protein interactions led to protein aggregation, resulting in a decreased *E* value.[32,33] After reaching fermentation and later (Fig. 3b), the value of the mucus *E* added to the SSHP gradually increased and exceeded the control group. The gut microbiota continuously utilized the nutrients in the system to catabolize polysaccharides of macromolecules. At this time, the sugar molecules may have bound to the proteins adsorbed by the interface through electrostatic interactions and hydrogen bonding.[34] This effect was weaker than covalent bond energy, and its adsorption was indirect; the molecular layer of polysaccharides was wrapped around the contact surface to form the interface. When the intensity increased, the adsorption behavior was enhanced, and the final *E* value was increased. These results may be biologically significant because they indicated differences in the

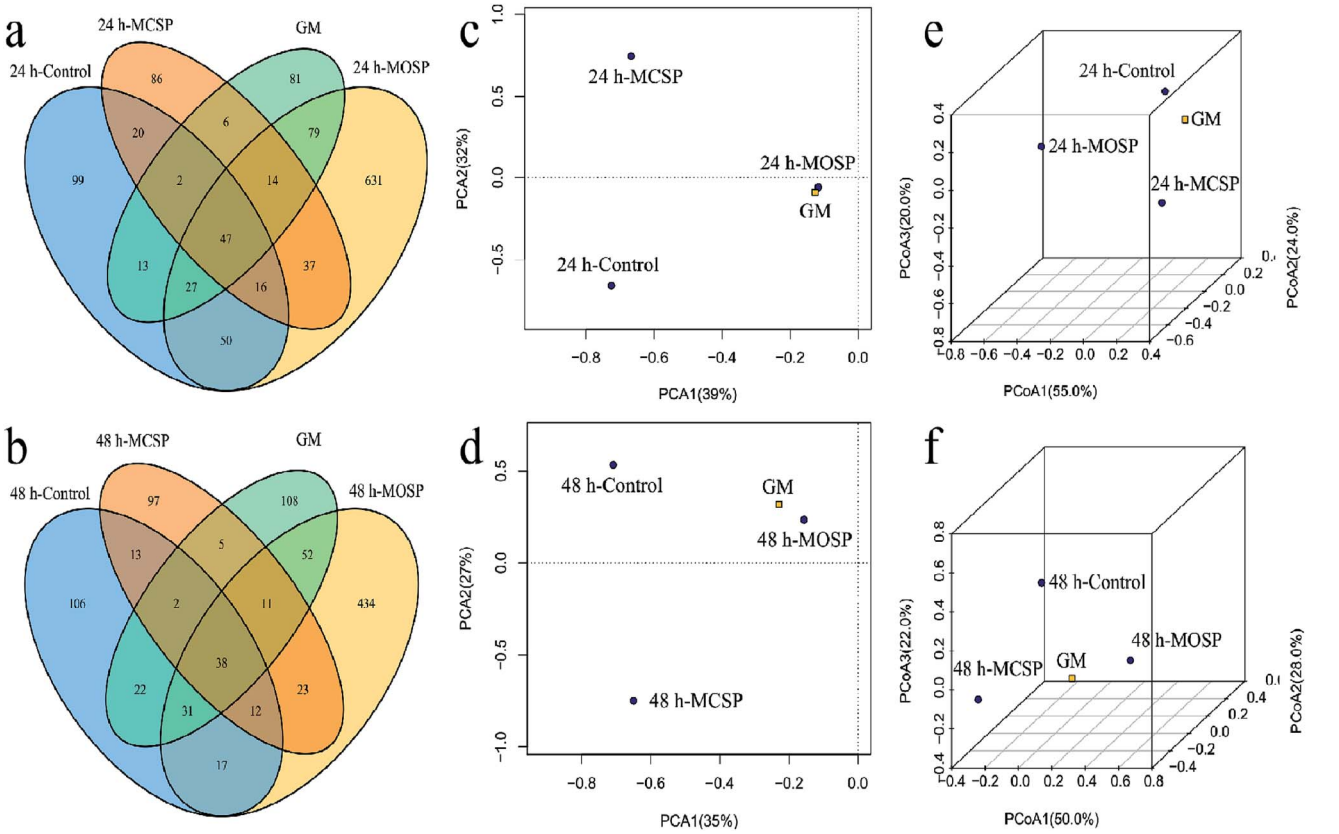

Fig. 4 Response of gut microbiota to SSHP treatment at different fermentation times (24 h and 48 h). (a and b) Effect of MCSP and MOSP treatment on OTUs of gut microbiota at 24 h and 48 h. (c and d) PCA score plot of the gut microbiota in all groups at 24 h and 48 h. (e and f) 3D-PCoA of the gut microbiota based weighted UniFrac metric at 24 h and 48 h.

performance of the intestinal flora in different mucus interactions. This difference was related to the type of polysaccharide and molecular weight. Guri[6] used interfacial dilation rheology to study the interaction between human intestinal mucus, milk protein, and epigallocatechin-3-gallate (EGCG). The results showed that polymer components and their complexes significantly affected the viscoelasticity of mucus. Although the presence of EGCG did not significantly affect the adsorption of milk protein and mucin at the interface, EGCG promoted an increase in surface membrane elasticity by interaction with milk proteins and mucin. Comparison of the elastic modulus of dilational also showed that there was a significant difference between the mixed interface and the mucus interface alone, indicating a change of physical properties caused by the interaction between mucus and the nutrients. Rossetti[35,36] studied the interaction of proteins in human saliva with different polyphenols during oral digestion, which influenced the air–liquid interface dilational characteristics. The complexity of salivary membrane kinetics and swelling surface rheology were also characterized. The results showed that the protein components with smaller molecular weight adsorbed at the interface to produce a solute-like surfactant reaction, while the adsorption of larger molecular weight proteins made the interface more difficult to dissolve. Thereafter, surface elastic changes of the preadsorbed saliva membrane in the polyphenol solution were measured, and it was confirmed that the chemical structure of the polyphenol molecule was a key factor affecting protein complexes.

The intake of SSHP changed the structure of the gut microbacterial community

To further understand the interaction of polysaccharides, mucus, and gut microbiota, we used high-throughput sequencing spanning the V3–V4 hypervariable regions of 16S rDNA. After quality control, a total of 368 656 high quality sequences were read for estimation. The values of Chao1 and ACE indices were positively correlated with richness of gut microbiota, and the Shannon index was positively correlated with diversity, while the Simpson index was negatively correlated with diversity (Table 4). MOSP effectively increased the richness and diversity of human gut microbiota compared to MCSP and the control. Fu[37] found that *Dendrobium officinale* polysaccharides significantly increased the Shannon index and OTUs of gut microbiota *in vitro*. Ding[38] also found that the *Lycium barbarum* polysaccharide community diversity and abundance of gut microbiota *in vitro* were comparable to carbon-free source groups and the inulin group.

Table 4 Effect of SSHP on diversity of fecal microbiota in mucus at different fermentation time

		Richness estimator		Diversity estimator	
Groups	Reads	Ace	Chao1	Shannon	Simpson
GM	57 859	372.22	337.96	2.70	0.16
24 h-control	51 456	524.31	389.11	2.00	0.30
24 h-MCSP	53 603	502.72	331.06	1.58	0.29
24 h-MOSP	56 071	966.73	952.94	3.00	0.09
48 h-control	47 688	345.73	320.33	2.28	0.23
48 h-MCSP	45 579	329.62	294.24	1.92	0.23
48 h-MOSP	56 400	670.16	696.05	3.42	0.14

We developed a Venn diagram based on shared OTUs and performed principal component analysis (PCA) and 3D-principal coordinate analysis (3D-PCoA) (Fig. 4). The Venn diagram provided additional verification of our results, indicating that the number of OTUs in the MOSP group was significantly increased compared to the MCSP and control groups (Fig. 4a and b). When comparing the similarities and differences of gut microbiota community structures in different samples by PCA and 3D-PCoA, as shown in Fig. 5c and d, the PCA score plots at 24 h and 48 h, whether in the first principal component or on the second principal component, it had the microbiota community structure of the MOSP group that was different from the MCSP group, but close to the GM group. The closer the distance in the PCoA diagram, the more similar the flora structure between the samples (Fig. 4e, f). Zhao[39] showed using PCA analysis that *Flammulina velutipes* polysaccharide significantly altered the community structure of gut microbiota of mice. Sun[40] reported that PCA analysis of *Gracilaria lemaneiformis* polysaccharides improved the gut microflora structures of high fat diet mice.

The variation of microbial diversity and richness combined with the difference of rheological properties of the fermentation broth may be due to the high viscosity of the SSHP intervention system (Fig. 2), which reduced the inhibition rate of harmful factors on microorganisms. During the late fermentation period, the nutrient consumption was excessive and the supply was insufficient, which led to a decrease of the abundance and diversity of the gut microbiota. Studies have reported that different carbohydrates have a screening effect on the gut microbiota,[38,39] which is consistent with the results of the present study. If the combination of different types of carbohydrates was increased, it was possible to greatly increase the diversity of gut microbiota under *in vitro* simulated conditions.

SSHP modulated the gut microbiota at different taxonomic levels

We compared the composition of the gut microbiota at the level of the gate (Fig. 5a). The abundance of Proteobacteria and Firmicutes in the MCSP and MOSP groups increased significantly, while the abundance of Bacteroides decreased, but the degree of influence was different. Previous studies have shown that gut microbiota are part of the body's energy balance mechanism, especially Firmicutes and Bacteroides, which play an important role in regulating absorption, energy conversion, and glucose metabolism.[41] Firmicutes can participate in glycan degradation through the gpPULs glycan degradation system, fermenting nondigestible carbohydrates to produce short chain fatty acid. Meanwhile, compared with MCSP, there was also the presence of Bacteroides in MOSP, which was mainly degraded by susCH/susED of PULs. The system utilized polysaccharides to improve

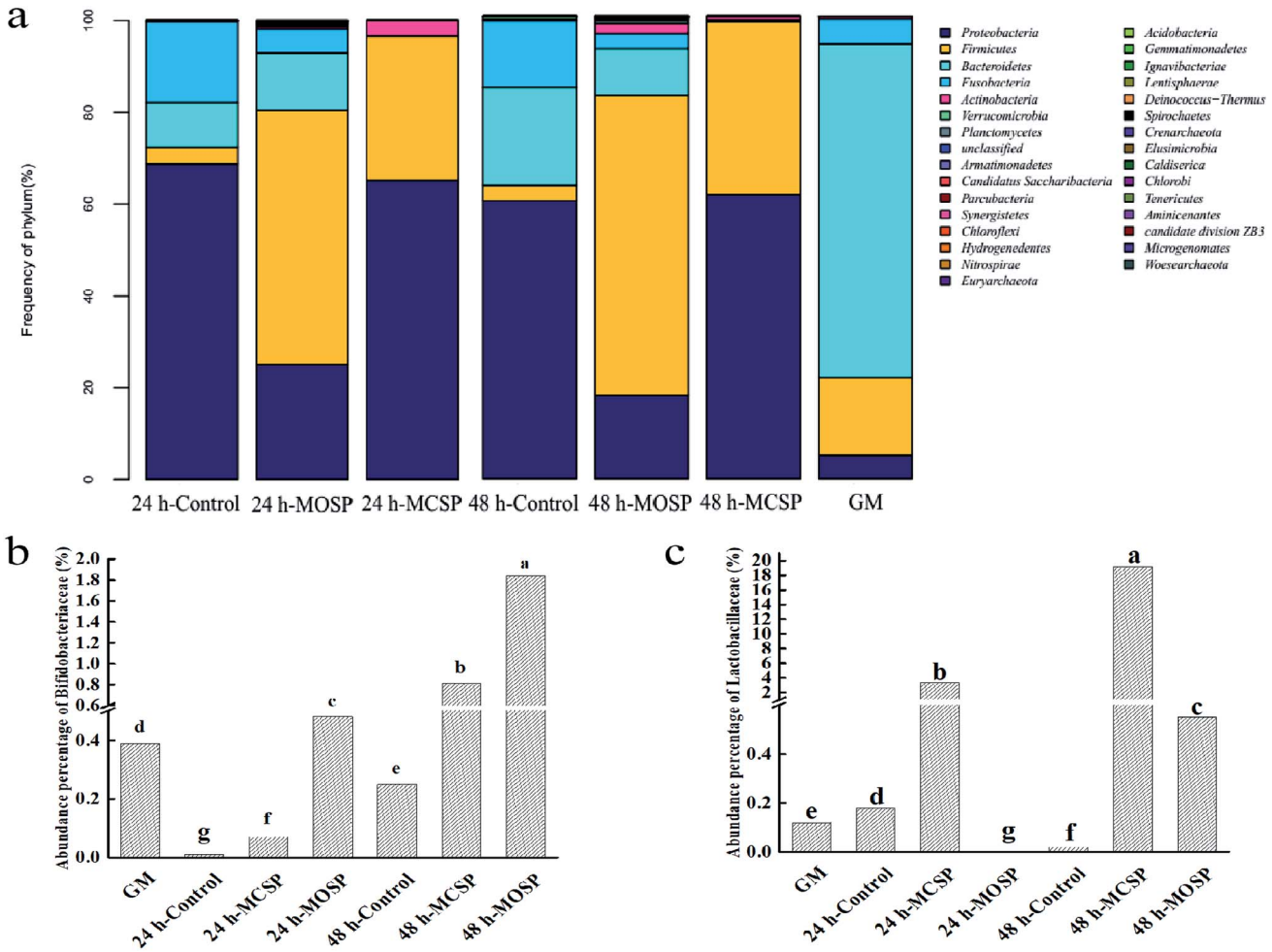

Fig. 5 Response of gut microbiota to SSHP treatment. (a) The relative abundances of the gut microbiota at the phylum levels. (b) The effect of SSHP on the abundance of Bifidobacteriaceae at the family level. (c) The effect of SSHP on the abundance of Lactobacillaceae at the family level.

the nutrient utilization of complex glycans and contributed to maintaining microecological balance.[9] It can be seen that MCSP and MOSP had a significant effect on improving the structural composition of the gut microbiota.

Next, we compared the bacterial composition of the gut microbiota at the family level and found that MCSP and MOSP had different effects on the abundance of Bifidobacteriaceae and Lactobacillaceae. Compared to the GM group, the abundance of Bifidobacteriaceae of the MOSP sample significantly increased after 24 h and 48 h of fermentation, but MCSP only significantly increased after 48 h of fermentation (Fig. 5b). The variation of Lactobacillaceae was significantly different from Bifidobacteriaceae. Compared to the GM group, the abundance of Bifidobacteriaceae of the MCSP group significantly increased after 24 h and 48 h of fermentation, but MOSP only significantly increased after 48 h of fermentation (Fig. 5c). These results indicated that Bifidobacteriaceae and Lactobacillaceae had different utilizations of SSHP, that MOSP had a better proliferation effect on Bifidobacteriaceae, and that MCSP had a more value-adding effect on Lactobacillaceae. Xu[42] found that *Porphyra haitanensis* polysaccharides significantly increased the abundance of Firmicutes and Proteobacteria of the intestinal tract, and that the structure of the intestinal flora was reshaped after 24 h of anaerobic culture. Xu[43] further showed that *Lactobacillus* spp. of mouse gut microbiota was enriched with feeding of *Ganoderma lucidum* polysaccharides. In addition, other studies have shown that polysaccharide fractions from the citrus shrub, *Fortunella margarita*, as a carbon source are superior to inulin and glucose in the proliferation of *Bifidobacterium*.[44] All the above results indicated that polysaccharides can be used as potential prebiotics. Moreover, studies have shown that *Bifidobacterium* and *Lactobacillus* not only do not degrade mucin glycoprotein, but also promote the secretion of intestinal mucin glycoprotein, and inhibit the adhesion of harmful bacteria such as *Escherichia coli* to mucous and intestinal epithelial cells.[45]

Conclusions

The macromolecule SSHP was degraded into reducing sugars and uronic acid by gut microbiota, causing a significant decrease in particle size. Therefore, the structure of mucus was destroyed, resulting in increased in viscoelasticity. Meanwhile, the proliferation of gut microbiota during the fermentation

process increased the viscosity of mucus. However, under the influence of gut microbiota, SSHP may first interact with intestinal mucus before being effectively transported and absorbed by intestinal cells. Meanwhile, SSHP increased the ratio of Proteobacteria to Firmicutes bacteria and promoted the growth of beneficial gut microbiota. However, MOSP promoted the proliferation of bifidobacteria, while MCSP promoted the abundance of lactic acid bacteria. The increase of probiotics abundance will conducive to improve the microecological balance, inhibit the growth of harmful bacteria, and maintain the health of the host. Therefore, the two polysaccharides have different effects on the structural composition of gut microbiota, which provides a research basis for the functional application of SSHP. The complexity of mucus–polysaccharide interaction plays an important role in polysaccharide intake, providing a theoretical basis for the development and utilization of SSHP.

Conflicts of interest

None.

Acknowledgements

This study was supported by the National Natural Science Foundation of China (Grant No. 31901680 and 31972031).

References

1 R. Clara, M. Schumacher, D. Ramachandran, S. Fedele, J. P. Krieger, W. Langhans and A. Mansouri, Metabolic Adaptation of the Small Intestine to Short- and Medium-Term High-Fat Diet Exposure, *J. Cell. Physiol.*, 2017, **232**, 167–175.

2 B. H. Bajka, N. M. Rigby, K. L. Cross, A. Macierzanka and A. R. Mackie, The influence of small intestinal mucus structure on particle transport ex vivo, *Colloids Surf., B*, 2015, **135**, 73–80.

3 S. Vicki, A. Adrian, P. W. Dettmar and J. P. Pearson, Colonic mucin: methods of measuring mucus thickness, *Proc. Nutr. Soc.*, 2003, **62**, 237–243.

4 M. Boegh, S. G. Baldursdottir, A. Mullertz and H. M. Nielsen, Property profiling of biosimilar mucus in a novel mucus-containing *in vitro* model for assessment of intestinal drug absorption, *Eur. J. Pharm. Biopharm.*, 2014, **87**, 227–235.

5 S. N. Warnakulasuriya and M. T. Nickerson, Review on plant protein-polysaccharide complex coacervation, and the functionality and applicability of formed complexes, *J. Sci. Food Agric.*, 2018, **98**, 5559–5571.

6 A. Guri, Y. Li and M. Corredig, Interfacial dilational properties of tea polyphenols and milk proteins with gut epithelia and the role of mucus in nutrient adsorption, *Food Funct.*, 2015, **6**, 3642–3651.

7 K. P. Scott, S. W. Gratz, P. O. Sheridan, H. J. Flint and S. H. Duncan, The influence of diet on the gut microbiota, *Pharmacol. Res.*, 2013, **69**, 52–60.

8 D. Ndeh and H. J. Gilbert, Biochemistry of complex glycan depolymerisation by the human gut microbiota, *FEMS Microbiol. Rev.*, 2018, **42**, 146–164.

9 D. W. Cockburn and N. M. Koropatkin, Polysaccharide Degradation by the Intestinal Microbiota and Its Influence on Human Health and Disease, *J. Mol. Biol.*, 2016, **428**, 3230–3252.

10 A. R. Mackie, A. Macierzanka, K. Aarak, N. M. Rigby, R. Parker, G. A. Channell, S. E. Harding and B. H. Bajka, Sodium alginate decreases the permeability of intestinal mucus, *Food Hydrocolloids*, 2016, **52**, 749–755.

11 H. Liu, X. Guo, J. Li, D. Zhu and J. Li, The effects of MgSO4, d-glucono-δ-lactone (GDL), sucrose, and urea on gelation properties of pectic polysaccharide from soy hull, *Food Hydrocolloids*, 2013, **31**, 137–145.

12 M. Dubois, K. A. Gilles, J. K. Hamilton, P. A. Rebers and F. Smith, Colorimetric Method for Determination of Sugars and Related Substances, *Anal. Chem.*, 1956, **28**, 350–356.

13 G. L. Miller, Dinitrosalicylic Acid Reagent for Determination of Reducing Sugar, *Anal. Biochem.*, 1959, **31**, 426–428.

14 N. Blumenkrantz and G. Asboe-Hansen, New method for quantitative determination of uronic acids, *Anal. Biochem.*, 1973, **54**, 484–489.

15 Y. Li, E. Arranz, A. Guri and M. Corredig, Mucus interactions with liposomes encapsulating bioactives: interfacial tensiometry and cellular uptake on Caco-2 and cocultures of Caco-2/HT29-MTX, *Food Res. Int.*, 2017, **92**, 128–137.

16 L. Yun, D. Li, L. Yang and M. Zhang, Hot water extraction and artificial simulated gastrointestinal digestion of wheat germ polysaccharide, *Int. J. Biol. Macromol.*, 2019, **123**, 174–181.

17 Y. Wang, G. Chen, Y. Peng, Y. Rui, X. Zeng and H. Ye, Simulated digestion and fermentation *in vitro* with human gut microbiota of polysaccharides from Coralline pilulifera, *LWT–Food Sci. Technol.*, 2019, **100**, 167–174.

18 H. Y. Zhang, Effects of Different Extraction Processes on the Structure of Soy Hull Polysaccharide, PhD diss., BoHai University, China, 2019.

19 L. Tang, Y. Chen, Z. Jiang, S. Zhong, W. Chen, F. Zheng and G. Shi, Purification, partial characterization and bioactivity of sulfated polysaccharides from Grateloupia livida, *Int. J. Biol. Macromol.*, 2017, **94**, 642–652.

20 J. Ahmed, S. Al-Jassar and L. Thomas, A comparison in rheological, thermal, and structural properties between Indian Basmati and Egyptian Giza rice flour dispersions as influenced by particle size, *Food Hydrocolloids*, 2015, **48**, 72–83.

21 S. K. Lai, Y. Y. Wang, D. Wirtz and J. Hanes, Micro- and macrorheology of mucus, *Adv. Drug Delivery Rev.*, 2009, **61**, 86–100.

22 H. Bokkasam, M. Ernst, M. Guenther, C. Wagner, U. F. Schaefer and C. M. Lehr, Different macro- and micro-rheological properties of native porcine respiratory and intestinal mucus, *Int. J. Pharm.*, 2016, **510**, 164–167.

23 H. Lazaro, L. Puente, M. C. Zúñiga and L. A. Muñoz, Assessment of rheological and microstructural changes of

soluble fiber from chia seeds during an *in vitro* micro-digestion, *LWT–Food Sci. Technol.*, 2018, **95**, 58–64.

24 N. Repin, S. W. Cui and H. D. Goff, Rheological behavior of dietary fibre in simulated small intestinal conditions, *Food Hydrocolloids*, 2018, **76**, 216–225.

25 A. Tamargo, C. Cueva, M. D. Álvarez, B. Herranz, B. Bartolomé, M. V. Moreno-Arribas and L. Laguna, Influence of viscosity on the growth of human gut microbiota, *Food Hydrocolloids*, 2018, **77**, 163–167.

26 L. Wang, H. M. Liu, C. Y. Zhu, A. J. Xie, B. J. Ma and P. Z. Zhang, Chinese quince seed gum: flow behaviour, thixotropy and viscoelasticity, *Carbohydr. Polym.*, 2019, **209**, 230–238.

27 S. Razmkhah, S. M. A. Razavi and M. A. J. Mohammadifar, Dilute solution, flow behavior, thixotropy and viscoelastic characterization of cress seed (Lepidium sativum) gum fractions, *Food Hydrocolloids*, 2017, **63**, 404–413.

28 D. R. Chejara, S. Kondaveeti, K. Prasad and A. K. Siddhanta, Studies on the structure–property relationship of sodium alginate based thixotropic hydrogels, *RSC Adv.*, 2013, **3**, 15744–15751.

29 E. Schultheis, M. A. Dreger, J. M. Muñoz-Villegas, J. I. Escalante, E. Franco-Lara and B. Nörtemann, Rheological characterization of culture broth containing the exopolysaccharide PS-EDIV from Sphingomonas pituitosa, *Biochem. Eng. J.*, 2009, **47**, 116–121.

30 A. M. Hernandez-Penaranda, J. A. Salazar-Montoya, R. Rodriguez-Vazquez and E. G. Ramos-Ramirez, Rheological behavior of Phanerochaete chrysosporium broth during lignin degradation, *J. Environ. Sci. Health, Part A: Toxic/Hazard. Subst. Environ. Eng.*, 2001, **36**, 1983–1996.

31 O. E. Pérez, C. Carrera Sánchez, A. M. R. Pilosof and J. M. Rodríguez Patino, Surface dilatational properties of whey protein and hydroxypropyl-methyl-cellulose mixed systems at the air–water interface, *J. Food Eng.*, 2009, **94**, 274–282.

32 R. A. Ganzevles, M. A. C. Stuart, T. V. Vliet and H. H. J. D. J. Jongh, Use of polysaccharides to control protein adsorption to the air–water interface, *Food Hydrocolloids*, 2006, **20**, 872–878.

33 P. Bertsch, A. Thoma, J. Bergfreund, T. Geue and P. Fischer, Transient measurement and structure analysis of protein-polysaccharide multilayers at fluid interfaces, *Soft Matter*, 2019, **15**, 6362–6368.

34 J. M. R. Patino and P. A. R. Pilosof, Proteine-polysaccharide interactions at fluid interfaces, *Food Hydrocolloids*, 2011, **25**, 1925–1937.

35 D. Rossetti, F. Ravera and L. Liggieri, Effect of tea polyphenols on the dilational rheology of human whole saliva (HWS): part 1, HWS characterization, *Colloids Surf., B*, 2013, **110**, 466–473.

36 D. Rossetti, F. Ravera and L. Liggieri, Effect of tea polyphenols on the dilational rheology of human whole saliva (HWS): part 2, polyphenols-HWS interaction, *Colloids Surf., B*, 2013, **110**, 474–479.

37 Y. Fu, J. Zhang, K. Chen, C. Xiao, L. Fan, B. Zhang, J. Ren and B. Fang, An *in vitro* fermentation study on the effects of Dendrobium officinale polysaccharides on human intestinal microbiota from fecal microbiota transplantation donors, *J. Funct. Foods*, 2019, **53**, 44–53.

38 Y. Ding, Y. Yan, Y. Peng, D. Chen, J. Mi, L. Lu, Q. Luo, X. Li, X. Zeng and Y. Cao, In vitro digestion under simulated saliva, gastric and small intestinal conditions and fermentation by human gut microbiota of polysaccharides from the fruits of Lycium barbarum, *Int. J. Biol. Macromol.*, 2019, **125**, 751–760.

39 R. Zhao, Q. Hu, G. Ma, A. Su, M. Xie, X. Li, G. Chen and L. Zhao, Effects of Flammulina velutipes polysaccharide on immune response and intestinal microbiota in mice, *J. Funct. Foods*, 2019, **56**, 255–264.

40 X. Sun, M. Duan, Y. Liu, T. Luo, N. Ma, S. Song and C. Ai, The beneficial effects of Gracilaria lemaneiformis polysaccharides on obesity and the gut microbiota in high fat diet-fed mice, *J. Funct. Foods*, 2018, **46**, 48–56.

41 A. Koliada, G. Syzenko, V. Moseiko, L. Budovska, K. Puchkov, V. Perederiy, Y. Gavalko, A. Dorofeyev, M. Romanenko, S. Tkach, L. Sineok, O. Lushchak and A. Vaiserman, Association between body mass index and Firmicutes/Bacteroidetes ratio in an adult Ukrainian population, *BMC Microbiol.*, 2017, **17**, 120.

42 S. Y. Xu, J. J. Aweya, N. Li, R. Y. Deng, W. Y. Chen, J. Tang and K. L. Cheong, Microbial catabolism of Porphyra haitanensis polysaccharides by human gut microbiota, *Food Chem.*, 2019, **289**, 177–186.

43 S. Xu, Y. Dou, B. Ye, Q. Wu, Y. Wang, M. Hu, F. Ma, X. Rong and J. Guo, Ganoderma lucidum polysaccharides improve insulin sensitivity by regulating inflammatory cytokines and gut microbiota composition in mice, *J. Funct. Foods*, 2017, **38**, 545–552.

44 P. Chen, Q. You, X. Li, Q. Chang, Y. Zhang, B. Zheng, X. Hu and H. Zeng, Polysaccharide fractions from Fortunella margarita affect proliferation of Bifidobacterium adolescentis ATCC 15703 and undergo structural changes following fermentation, *Int. J. Biol. Macromol.*, 2019, **123**, 1070–1078.

45 C. Kotzamanidis, A. Kourelis, E. Litopoulou-Tzanetaki, N. Tzanetakis and M. Yiangou, Evaluation of adhesion capacity, cell surface traits and immunomodulatory activity of presumptive probiotic Lactobacillus strains, *Int. J. Food Microbiol.*, 2010, **140**, 154–163.

